Environmental Science Nano

Accepted Manuscript

This article can be cited before page numbers have been issued, to do this please use: J. Yu, X. Wang, Q. Kang, J. Li, D. Shen and L. Chen, *Environ. Sci.: Nano*, 2016, DOI: 10.1039/C6EN00395H.

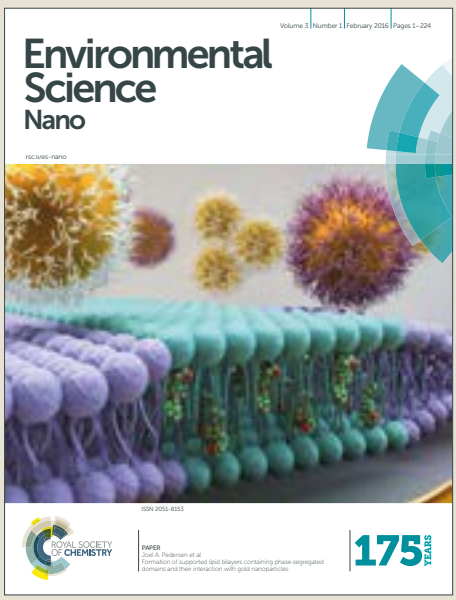

ROYAL SOCIETY OF CHEMISTRY

rsc.li/es-nano

View Article Online
DOI: 10.1039/C6EN00395H

Environmental significance statement

We propose a novel molecular imprinting fluorescence nanosensor via a facile surface imprinting polymerization one-pot synthesis strategy for highly selective and sensitive recognition and detection of 4-nitrophenol (4-NP) on the basis of electron transfer induced fluorescence quenching mechanism. By combining the high selectivity of molecularly imprinted polymers (MIPs) and the strong fluorescence property of quantum dots (QDs), the QD@MIPs nanosensor was demonstrated highly selective and sensitive towards 4-NP, with satisfactory rapidity, accuracy, reliability and practicality. This sensing platform is readily constructed in solution without any other labeling or modification steps, and demonstrated remarkable advantages such as simplicity, rapidity and universality, high selectivity and sensitivity, and good reliability and practicability. This work focuses on the microanalysis of trace 4-NP in complicated environmental water samples by using a kind of new high-effective nanoscale sensing material.

View Article Online
DOI: 10.1039/C6EN00395H

One-pot synthesis of quantum dots based molecular imprinting nanosensor for highly selective and sensitive fluorescent detection of 4-nitrophenol in environmental water

Jialuo Yu[a,b], Xiaoyan Wang[a,b,c], Qi Kang[a], Jinhua Li[b], Dazhong Shen[a,*], Lingxin Chen[b,*]

[a] *College of Chemistry, Chemical Engineering and Materials Science, Collaborative Innovation Center of Functionalized Probes for Chemical Imaging in Universities of Shandong, Key Laboratory of Molecular and Nano Probes, Ministry of Education, Shandong Provincial Key Laboratory of Clean Production of Fine Chemicals, Shandong Normal University, Jinan 250014, China*

[b] *Key Laboratory of Coastal Environmental Processes and Ecological Remediation, Yantai Institute of Coastal Zone Research, Chinese Academy of Sciences, Yantai 264003, China*

[c] *School of Pharmacy, Binzhou Medical University, Yantai 264003, China*

* Corresponding authors.

E-mail addresses: dzshen@sdnu.edu.cn (D. Shen), lxchen@yic.ac.cn (L. Chen).

View Article Online
DOI: 10.1039/C6EN00395H

ABSTRACT: A novel molecular imprinting fluorescence nanosensor was constructed via a facile surface imprinting polymerization one-pot synthesis strategy for highly selective and sensitive recognition and detection of 4-nitrophenol (4-NP) based on electron-transfer induced fluorescence quenching mechanism. 2-Aminoethyl methacrylate hydrochloride (AMA) was first used as a surfactant to interact with aqueous carboxyl-CdTe quantum dots (QDs) and the resultant AMA-modified QDs were used as core support and fluorescence signal source. Then, ultrathin 4-NP imprinted shell (ca. 4 nm) was formed on the QDs surface (i.e., QD@MIPs) by a simple facile free radical polymerization step. The one-pot synthesis simplified the imprinting process and shortened the experimental period. The imprinted sites bound the template of 4-NP efficiently through the hydrogen bonding interactions and showed excellent recognition selectivity for 4-NP over its analogues with a high imprinting factor of 9.1. The electron transfer process between QDs and 4-NP led to significant fluorescence quenching of the QD@MIPs nanosensor, by which 4-NP could be sensed, and high detection sensitivity up to 0.051 μM was attained. Furthermore, the sensor was successfully applied to determine 4-NP in seawater and lake water samples, presenting high recoveries in the range of 92.7–109.2% at three spiking levels with the relative standard deviation within 3.1–4.8%. The simple, rapid, reliable QD@MIPs based method proved potentially applicable for the highly selective and sensitive fluorescent determination of trace 4-NP in complicated environmental water samples.

***Keywords*:** Molecular imprinting, Quantum dots, One-pot synthesis, Fluorescent detection, 4-Nitrophenol, Environmental water

View Article Online
DOI: 10.1039/C6EN00395H

1. Introduction

With the development of chemical industry, a large number of refractory poisonous organic pollutants in industrial wastewater have been increasingly discharged to the environment. Nitrophenols are among the most common toxic persistent pollutants and widely used as the synthetic intermediates of pesticides, medicines, dyes, plastics and other fine chemicals and as the hydrolytic products of some organophosphorus insecticides.[1,2] 4-Nitrophenol (4-NP), a kind of common and important nitrophenol, has been listed as priority toxic pollutants by United States Environmental Protection Agency (EPA) due to its healthy and toxicological effects; a Lifetime Health Advisory (LHA) level of 60 μg/L for 4-NP in drinking water has been established.[3] Currently reported traditional detection methods for trace 4-NP mainly include spectrophotometry,[4,5] chromatographic techniques,[6] high-performance liquid chromatography,[7–9] electrochemical methods,[10,11] and capillary electrophoresis.[12,13] However, these methods often require extensive sample preparation and separation procedures, owing to the complexity of the sample matrices and the low content of 4-NP. Also, they still suffer from some problems such as complicated instruments, inconvenient derivatization and toxic derivatization reagents, high cost, time-consuming process, and particularly low selectivity.[14] Thus, it is important to develop simple, rapid, efficient approaches for the selective and sensitive determination of 4-NP.

In recent years, molecular imprinting has proven to be a versatile approach to the preparation of synthetic receptors with tailor-made recognition sites[15] and the resultant molecularly imprinted polymers (MIPs) can be used to separate and detect specific molecules quite effectively, along with low cost, easy preparation and high selectivity.[16] The typical MIPs are polymerized by functional monomers, cross-linkers and polymerization initiators in the presence of the templates in the solvents. After the removal of the template, recognition sites complementary in size, shape, and functionality to the template are formed in the 3D

View Article Online
DOI: 10.1039/C6EN00395H

polymer network.[17] Traditional MIPs are usually prepared by bulk imprinting but have many disadvantages including poor binding capacity, incomplete template removal and low binding kinetics,[18] due to their shells too thick to extract the template molecules completely. To overcome these limits, recently, surface imprinting technique has been employed for preparing MIPs, by which recognition sites can be formed on the material surface.[19] Furthermore, core–shell structural surface imprinted polymers have shown the superiority of excellent selectivity, faster mass transfer, better synthesis reproducibility and improved binding capacity.

On the other hand, MIP-based fluorescence sensors have been increasingly developed owing to their high selectivity and sensitivity for detection of low contents target analytes from complex samples.[20] Semiconductor nanocrystal quantum dots (QDs), with their excellent photostability, size-tunability, a broad range of excitation wavelengths and narrow luminescence spectra and chemically functional surfaces, have been widely used as fluorescence labels.[21–23] The MIP-based QDs fluorescent sensors have played important parts in detecting various trace analytes, which combine the merits of high selectivity of MIPs recognition and high sensitivity of fluorescence detection.[24,25] Usually, the construction of MIP-based QDs sensors requires using matrixes (e.g., silica) as substrates or embedding QDs into highly cross-linked MIPs. However, this will make the fluorescence of QDs become weak and thereby reduce the sensing sensitivity, along with the laborious and time-consuming process.[26,27] So, without matrixes and embedding is highly desirable to develop MIP-based QDs sensors.

Therefore, herein, via direct imprinting on QDs surface without using the common matrix materials or embedding process, we developed a simple facile one-pot synthesis strategy to construct a novel MIP-based QDs sensor namely QD@MIPs for 4-NP determination. 2-Aminoethyl methacrylate hydrochloride (AMA) was employed as a

View Article Online
DOI: 10.1039/C6EN00395H

polymerizable surfactant to coat the carboxyl-CdTe QDs by electrostatic interaction, and thus the aqueous QDs were firmly stabilized and showed strong fluorescence. Then the QDs were used as support materials and fluorescent signal source, and ultrathin imprinted shell was prepared on QDs surface by facile free radical polymerization process using 4-NP as template, acrylamide as functional monomer and N,N'-methylenebisacrylamide (MBA) as cross-linker. The constructed QD@MIPs sensor was well characterized and its recognition/sensing properties were investigated in detail. The developed QD@MIPs based sensing method was validated and successfully applied for the selective and sensitive detection of 4-NP in seawater and lake water samples.

2. Experimental

2.1. Reagents and materials

2-Aminoethyl methacrylate hydrochloride (AMA) was purchased from Sigma-Aldrich (Shanghai, China). Absolute ethanol, acetonitrile, sodium hydroxide (NaOH), Tellurium powder, cadmium nitrate ($Cd(NO_3)_2$), thioglycollic acid (TGA), 4-nitrophenol (4-NP), phenol, nitrobenzene (NB), 2-nitrophenol (2-NP), acrylamide (AAM), potassium persulfate and phosphate buffered saline were supplied by Sinopharm Chemical Reagent Co. Ltd. (Shanghai, China). N,N'-methylenebisacrylamide (MBA), sodium borohydride ($NaBH_4$) and bisphenol A (BPA) were obtained from Aladdin (Shanghai, China). Estradiol and 4-chlorophenol (4-CP) were purchased from J&K Technology Ltd. (Beijing, China).

2.2. Instrumentation

Fluorescence measurements were taken on a Fluoromax-4 Spectrofluorometer (Horiba Scientific), and the fluorescence lifetimes were measured on an Edinburgh OB920FP fluorescence and phosphorescence lifetime spectrometer. UV-vis spectra were measured on a Thermo Scientific NanoDrop 2000/2000C spectrophotometer (Thermo Fisher Scientific,

View Article Online
DOI: 10.1039/C6EN00395H

Waltham, MA). The morphological evaluation was recorded by a transmission electron microscopy (TEM, JEM-1230, operating at 100 kV). Zeta potential and dynamic light scattering (DLS) measurements were performed on a Malvern Zetasizer Nano-ZS90 (ZEN3590, UK). Energy dispersive spectrum (EDS) was measured by a scanning electron microscope (SEM, Hitachi S-4800 FE-SEM, operating at 5 kV) equipped with an EDAX-PHOE-NIX energy spectrum probe. Elemental analysis was performed using a Vario Micro-cube elementar analyzer (Elementar Company, Germany). FT-IR analyses were carried out by a FT-IR spectrometer (Thermo Nicolet Corporation, USA).

2.3. One-pot synthesis of MIP-based QDs sensor

One-pot synthesis strategy was utilized to construct a MIP-based QDs sensor. Firstly, green emissive TGA-modified CdTe QDs were synthesized in aqueous phase according to a reported method[17] with slight modification. Briefly, 40 mg of $NaBH_4$ and 38.3 mg of tellurium powder were added to 1.5 mL absolute ethanol and 0.5 mL ultrapure water to form a mixture, which was reacted for 4 h in 40 ºC. 92.4 mg of $Cd(NO_3)_2{\cdot}4H_2O$ and 63 μL of TGA were dispersed in 75 mL of ultrapure water, and the pH value of the solution was then adjusted to 9 with 1.0 M NaOH. The solution mixture was deoxygenated by purging nitrogen for at least 30 min. Next, 1 mL of freshly prepared NaHTe aqueous solution was transferred into the above mixture under stirring. After boiling and refluxed for 2 h, the green emissive TGA-modified CdTe QDs were obtained.

Then, AMA modification was carried out and the surface imprinting sensor based on AMA-modified CdTe QDs, marked as QD@MIPs, was prepared via a facile free radical polymerization process. Briefly, 200 μL of AMA solution (1 $g{\cdot}L^{-1}$) and 5 mL of aqueous CdTe QDs were added to 10 mL of ultrapure water under vigorously stirring for 1 h. Subsequently, 5 mg of 4-NP, 10 mg of AAM and 5 mg of MBA were dissolved in this solution for pre-polymerization. After purged with N_2 for 30 min, 4 mg of potassium persulfate was added,

View Article Online
DOI: 10.1039/C6EN00395H

and kept stirring at 40 ºC overnight in the dark. Finally, the products were centrifuged and washed with ethanol/acetonitrile (8:2, v/v) to remove 4-NP, and then washed with ultrapure water for three times. The resultant QD@MIPs were dispersed in 3 mL of ultrapure water for further use. As a control, the non-imprinted polymers (QD@NIPs) were prepared in the same manner but without adding template 4-NP.

2.4. Fluorescence measurement

All the fluorescence (FL) intensities were measured under the same conditions: the excitation and emission slit widths were both 6 nm and the excitation wavelength was set at 420 nm with a recording emission range of 440–700 nm. QD@MIPs and QD@NIPs were added into the 4-NP solutions at known concentrations and the final concentration of MIPs or NIPs was 0.02 $mg \cdot mL^{-1}$. Before measurement, the lamp intensity was calibrated.

2.5. Analysis of water samples

Water samples were utilized to examine the practical applicability of the QD@MIPs for the detection of 4-NP. Seawater samples were randomly collected from the surface seawater of Yellow Sea and lake water samples were acquired from San Yuan Lake, located in the coastal zone region of Yantai City. And the water samples were all filtered with 0.45 μm microfiltration membrane to remove the suspended particles before use. The spiked seawater and lake water samples diluted 100-fold with different concentrations of 4-NP were used to validate the accuracy and applicability of the QD@MIPs.

3. Results and discussion

3.1. Preparation and possible sensing principle of QD@MIPs

Fig. 1 illustrates the preparation process of QD@MIPs. As seen, aqueous carboxyl-CdTe QDs, used as core support materials and fluorescent signal source, was firstly stabilized by modifying AMA. The zeta potential of CdTe QDs solution increased significantly from –30.1

View Article Online
DOI: 10.1039/C6EN00395H

to –19.3 mV indicated that the negatively charged CdTe QDs easily interact with the positively charged AMA for the formation of the desired structure by electrostatic attraction.[28,29] The polymerizable surfactant AMA provided the isopropenyl on the QDs surface which played a key role to copolymerize with AAM and MBA. Then the 4-NP imprinted shell was formed on the surface of AMA-modified QDs nanoparticles by one simple facile free radical polymerization step, using AAM as functional monomer, MBA as cross-linker, and potassium persulfate as initiator. After removing the embedded template 4-NP, the QD@MIPs with specific imprinted cavities (sites) were obtained. The MIPs shell layer could not only protect the fluorescence of QDs and effectively decrease QDs toxicity but also facilitate high accessibility into binding sites and rapid mass transfer of template molecules.

Also, Fig. 1 schematically shows the recognition process and possible sensing principle for 4-NP by the prepared QD@MIPs. As seen, the electron-rich amino group at the surface of the imprinted sites would efficiently bind the hydroxyl group of template 4-NP through the strong hydrogen bonding interactions. The fluorescence quenching could be attributed to the electron transfer between QDs and 4-NP. As seen from Fig. S1A, the electrons of QDs were excited from the ground state (valence band) to the conduction band and transited to the initial condition to generate the green emission (Fig. S1A (a)). The UV-vis absorption of 4-NP and 4-NP ion was at around 229, 316 and 415 nm, respectively (Fig. S1B (b)), which is near to the band gap of the QDs as revealed by the absorption spectra of the QD@MIPs (Fig. S1B (c)). Thus, with the existence of 4-NP, the electrons at the conductive band of the QDs could directly transfer to the lowest unoccupied molecular orbital (LUMO) of UV and the visible band of the 4-NP molecules or ions.[30] Since all the energy bands of the 4-NP molecules and 4-NP ions were higher than the emission of QDs, the excited electrons of QDs tended to go back to the ground state without emitting fluorescence, which would lead to the fluorescence

View Article Online
DOI: 10.1039/C6EN00395H

quenching of QDs, as illustrated in Fig. S1A (b). Meanwhile, the absorption spectrum of 4-NP had no spectral overlap with the emission spectrum of CdTe QDs, as shown in Fig. S1B. Therefore, we concluded the energy transfer wouldn't be the dominant mechanistic pathway and further confirmed that the fluorescence quenching behavior was due to the electron transfer process. As is well known, fluorescence quenching generally includes dynamic quenching and static quenching. Fluorescence lifetime measurements experiments are often carried out to identify the type and mechanism of quenching. The average lifetime of QD@MIPs was attained of 15.93 ns and the lifetime of QD@MIPs with the presence of 4-NP was 15.37 ns. That the lifetime of QD@MIPs was almost unchanged upon 4-NP addition could indicate the quenching belongs to static quenching.[31] On the other hand, the comparison in lifetime values of QD@MIPs (15.93 ns) with that of QDs (20.00 ns) and QD@NIPs (18.32 ns) suggested that the polymeric shell in the nanoparticles surface has not significant influence on the parameter. Consequently, a new QD@MIPs sensor was prepared, and it could recognize and detect 4-NP fluorescently based on electron transfer induced static fluorescence quenching mechanism.

Fig. 1.

3.2 Characterization of the QD@MIPs

The morphological structures of QDs, QD@MIPs and QD@NIPs were investigated by TEM. As shown in Fig. S2A, CdTe QDs nanoparticles had good dispersion with the average diameter of ca. 1–2 nm. The QD@MIPs and QD@NIPs had similar morphology and also exhibited good dispersion (Fig. S2B and S2C). The imprinting shell thickness was ca. 4 nm, which provided excellent imprinting sites on the modified QDs surface for special recognition. The size distribution of nanoparticles was obtained by DLS measurement as depicted in Fig. S3. It tends to overestimate the diameters of nanoparticles measured by TEM images because

View Article Online
DOI: 10.1039/C6EN00395H

DLS measured hydrodynamic diameters. The intensity contribution versus diameters of nanoparticles displayed a good size-distribution, and most of the hydrodynamic diameter of QDs was found to be < 4 nm (Fig. S3A), and the dominant distribution peak of QD@MIPs and QD@NIPs were around 8 nm (Fig. S3B and S3C). In addition, the quite low ratio size-distribution of large diameters also suggested the slight agglomeration of the nanoparticles, which is consistent with TEM results (Fig. S2D–F). Overall, therefore, the ultrathin imprinting shell layer could contribute shorter response time and higher sensitivity for the nanosensor.

EDS analysis was carried out to confirm the nature of the surface modification of the CdTe precursor nanoparticle, as recorded in Fig. S4 and Table S1. The presence of S, Te and Cd suggested the TGA modified CdTe QDs were used as support material for surface modification to produce QD@MIPs and QD@NIPs. The obviously increased percentages of both carbon (46.34%) and oxygen (36.35%) for QD@MIPs, as well as carbon (35.56%) and oxygen (34.50%) for QD@NIPs, might well result from the subsequently coated polymer materials, and suggested the occurrence of imprinting. Furthermore, elemental analysis was performed to examine nitrogen content. The marked enlargement in the nitrogen atomic composition from 0.203% for QDs to 1.06% for QD@MIPs revealed that amine groups were successfully introduced onto the surface of QDs. Meanwhile, imprinting proved to play an important role when compared to the nitrogen ratio (0.688%) for QD@NIPs. These experimental data were able to provide direct evidences on the chemical modification of particles.

The fluorescence spectra of QDs, AMA-modified QDs and QD@MIPs were displayed in Fig. 2. As seen, the fluorescence intensity of the CdTe QDs (Fig. 2(a)) was reduced by 2.7% after modification of AMA (Fig. 2(b)), which was mainly attributed to the electrostatic interaction between the QDs and AMA. After polymerization, the fluorescence spectra of

View Article Online
DOI: 10.1039/C6EN00395H

QD@MIPs showed a slight red shift and the fluorescence intensity partly decreased (Fig. 2(c)), in comparison with that of the AMA-modified QDs (Fig. 2(b)). This phenomenon can be explained as follows: a single charge close to the QDs surface could generate an electric field, and it was sufficiently large to cause fluorescence quenching and red shift.[17] Further, the resultant QD@MIPs could increase the effective size of the QDs and reduce the quantum size effect, which would cause a red shift of the photoluminescence maximum.[26] The results clearly suggested that the QD@MIPs fluorescence sensor was attained.

Fig. 2.

The FT-IR spectra of QDs, QD@MIPs and QD@NIPs were shown in Fig. 3. It can be found that the QD@MIPs and QD@NIPs showed similar locations of the major bands owing to the same composition. As seen from Fig. 3(b) and 3(c), the peaks at around 1646 cm^{-1} could be assigned as the C=O bond vibration from amide band and the bands at 1260 cm^{-1} could be attributed to the stretching vibration of C–N. Meanwhile, the characteristic peaks of amino groups were around 1554 cm^{-1}, verifying the introduction of amine ligand. All the bonds further confirmed that the QD@MIPs nanosensor was successfully fabricated by the composing of AMA, AAM and MBA at the surface of QDs nanoparticles.

Fig. 3.

3.3 Condition optimization on fluorescence properties of the QD@MIPs sensor

Condition optimization on the fluorescence properties of QD@MIPs sensor was performed mainly including solution acidity and response time as follows. Fig. 4A shows the effects of pH on fluorescence quenching capacity of QD@MIPs in the presence of 4-NP. The quenching efficiency, defined as $(F_0–F)/F_0$, was used as the index of quenching capacity. It is known to all, high acidity will affect the fluorescence intensity of CdTe QDs, especially, when

View Article Online
DOI: 10.1039/C6EN00395H

the pH≤4, the fluorescence intensity of CdTe QDs can be quenched totally.[32] On the other hand, high alkalinity will intensively destroy the interaction between 4-NP and imprinting sites. So, the pH range of 6.0–9.0 was tested. As shown in Fig. 4A, when the solution pH increased from 6.0–7.0, fluorescence quenching efficiency increased obviously, and then changed slightly within the pH of 7.0–9.0. The increasing quenching efficiency is very likely owing to the high fluorescence efficiency of QDs[33] and strong binding of imprinting sites towards 4-NP. In the range of pH 7.0–9.0, pH had slight influence on fluorescence intensity of the QD@MIPs, which made the sensor suitable for potential applications in real water samples as the environmental water samples are usually (near) neutral or slightly alkaline. For convenience, hence, subsequent experiments were carried out at pH 7.5.

The response time of the QD@MIPs sensor was also tested in order to assess the accessibility to binding sites. As shown from Fig. 4B, within 0−5.5 min, the fluorescence intensity decreased significantly, while within 5.5−8 min the decrease amounts became small, after which the curve became flat and equilibrium was reached. The short response time could be attributed to the thin imprinting layer of the QD@MIPs sensor, which offered fast mass transfer and high site accessibility toward the template. Under our experimental conditions, a stable fluorescence intensity was reached after a response time of 8 min. Accordingly, 8 min was chosen as the response time in further experiments for the determination of 4-NP.

Fig. 4.

3.4 Sensitivity and selectivity of the QD@MIPs sensor

Under the optimal conditions, the ability of the QD@MIPs sensors for quantitative determination of 4-NP was further evaluated. In this system, the fluorescence quenching followed the Stern−Volmer equation[34]

$$F_0/F = 1 + K_{sv}C_q$$

View Article Online
DOI: 10.1039/C6EN00395H

where F_0 and F are the fluorescence intensity of QDs in the absence and presence of the quencher, respectively, K_{sv} is the Stern−Volmer quenching constant, and C_q is the quencher concentration. Herein, the ratio of $K_{sv,MIP}$ to $K_{sv,NIP}$ was defined as the imprinting factor.

As shown in Fig. 5A, the fluorescence intensity of QD@MIPs was quenched gradually with the increasing of 4-NP concentrations, presenting an excellent linearity over the range of 0.2–8.0 μM with a correlation coefficient of 0.9998 (Inset of Fig. 5A). Based on $3\sigma/s$, in which σ is the standard deviation of the blank measurements and s is the sensitivity of the calibration graph, the limit of detection (LOD) was estimated to be 0.051 μM. The value is much lower than the LHA level of 60 μg/L (0.43 μM) for 4-NP in drinking water regulated by EPA.[3] Therefore, the developed QD@MIPs sensor holds great potentials as an ideal alternative to determination of trace 4-NP in real water samples for pollution monitoring. On the contrast, as seen in Fig. 5B, the fluorescence intensity of QD@NIPs only slightly decreased at the same concentration of 4-NP. Consequently, a high imprinting factor could be obtained of 9.1. The decrease of fluorescence intensity of QD@MIPs sensor was much larger than that of QD@NIPs, which suggested that the presence of MIPs layers greatly enhanced the quenching efficiency and thereby enlarged the spectral sensitivity to 4-NP owing to the formation of specific recognition sites in the QD@MIPs with predetermined selectivity toward 4-NP.

Fig. 5.

Meanwhile, the selectivity of the MIPs sensor was investigated by measuring the fluorescent response of QD@MIPs toward 4-NP and its analogues including phenolic compounds such as 2-NP, 4-CP, phenol, BPA and estradiol and nitro-compounds such as NB. As seen from Fig. 6, fluorescence quenching amount of the QD@MIPs was the highest for 4-NP, followed by 2-NP and 4-CP, larger than NB, phenol, BPA and estradiol which caused

View Article Online
DOI: 10.1039/C6EN00395H

very close and quite low fluorescence quenching. In the synthesis process, a larger number of specific imprinting/recognition sites complementary with the template molecules in shape, size, and functionality were generated on the MIPs; hence the template 4-NP could be strongly rebound to the MIPs and then produce significant fluorescence quenching. As for 2-NP, its spatial structure is different from 4-NP; as for 4-CP, its electron-withdrawing property of chlorin group is weaker than that of nitro groups. So, the 2-NP and 4-CP molecules would partly bind the imprinting sites, resulting in certain fluorescence quenching. This observation for NB with quite low fluorescence quenching amounts might be ascribed that the NB does not contain the functional group of hydroxyl and thereby producing very weak binding with imprinting sites. As for phenol, BPA and estradiol, much different from 4-NP in size and spatial structure, they were not complementary to the recognition sites and thereby had less chance to access. So, it is quite difficult to quench QDs fluorescence. Consequently, the QD@MIPs sensor had high selectivity toward the template 4-NP. In contrast, the QD@NIPs sensor showed similar and quite low fluorescence quenching for 4-NP and the six possibly interfering compounds. Hence, the molecularly imprinted nanosensor could be applied to the selective detection of 4-NP.

Fig. 6.

3.5. Practical application of the sensor to environmental water samples

In order to further evaluate the practical applicability of the MIPs sensor, 4-NP was detected by the QD@MIPs in real water samples diluted 100-fold spiked with different concentrations of 4-NP, including seawater and lake water. The averaged recovery was obtained with relative standard deviation (RSD) based on three triplicate measurements for each concentration. As listed in Table 1, satisfactory recoveries were attained in a range of 92.7−106.0% with RSDs of 3.1−4.8% for the spiked seawater samples. As well as, the

View Article Online
DOI: 10.1039/C6EN00395H

recoveries for the spiked lake water samples were 102.3−109.2% with RSDs of 3.4−4.7%. The results indicated that the MIPs sensor was feasible for accurate determination of trace 4-NP in complex environmental water samples, possessing great potential for practical applications.

Table 1.

3.6 Method performance comparison

The performance of the developed fluorescence nanosensor for detection of 4-NP was compared with that of some reported methods, as listed in Table 2.[14,35−39] As seen from the table, all the systems are based on fluorescence quenching, which results from electron transfer or energy transfer from the fluorescent labels to 4-NP, owing to the possible formation of hydrogen bonds. The fluorescence sources/labels, such as carbon dots[35] can be directly used to detect 4-NP with high sensitivity but low selectivity due to the fluorescence quenching by some metal ions or other structure analogs. Most of the MIPs based fluorescent materials are prepared by the Stöber method,[14,36,37,39] and interestingly we firstly present a facile one-pot synthesis strategy for preparing QD@MIPs fluorescence nanosensor with higher sensitivity. Although our attained sensitivity is slightly lower than that reported,[35,38] excitingly, the imprinting factor of 9.1 was much higher than others,[14,37−39] which indicated a super selectivity of the developed nanosensor. Also, the QD@MIPs nanosensor was successfully applied to determine 4-NP in seawater and lake water samples. Therefore, overall, the present analytical method in our study offers remarkable advantages such as convenience, rapidity and universality, high sensitivity and selectivity, and good reliability and practicability.

Table 2.

View Article Online
DOI: 10.1039/C6EN00395H

4. Conclusions

In conclusion, a novel QD@MIPs nanosensor for fluorescent determination of trace 4-NP in environmental water samples based on electron-transfer induced fluorescence quenching mechanism, was successfully developed by a facile surface imprinting polymerization one-pot synthesis strategy. By combining the high selectivity of MIPs and the strong fluorescence property of QDs, the nanosensor was demonstrated highly selective and sensitive towards 4-NP, with satisfactory rapidity, accuracy, reliability and practicality. Besides, this sensing system provided other advantages and possible inspirations: (1) The use of a simple, inexpensive commercially available AMA containing both amino group and isopropenyl offers direct imprinting and avoids any design/synthesis or using matrix materials or embedding process. (2) This sensing platform is readily constructed in solution without any other labeling or modification steps. (3) With the fast development of versatile MIPs and gradual concern for QDs or other signal sources, more efforts still need to be made to develop high-performance composite material based fluorescence sensors for potential applications such as water pollution monitoring and abatement.

Acknowledgments

This work was financially supported by the National Natural Science Foundation of China (21575080, 21275091, 21275158, 21477160), the National Defense Science and Technology Innovation Project of Chinese Academy of Sciences (CXJJ-16M254), and the Scientific Research Foundation for the Returned Overseas Chinese Scholars, State Education Ministry.

View Article Online
DOI: 10.1039/C6EN00395H

References

1 M. A. Oturan, J. Peiroten, P. Chartrin and A. J. Acher, Complete destruction of p-nitrophenol in aqueous medium by electro-Fenton method, *Environ. Sci. Technol.*, 2000, 34, 3474–3479.

2 Y. L. Zheng, D. Liu, H. Xu, Y. L. Zhong, Y. Z. Yuan, L. Xiong and W. X. Li, Biodegradation of p-nitrophenol by Pseudomonas aeruginosa HS-D38 and analysis of metabolites with HPLC–ESI/MS, *Int. Biodeter. Biodegr.*, 2009, 63, 1125–1129.

3 I. Tapsoba, S. Bourhis, T. Feng and M. Pontié, Sensitive and selective electrochemical analysis of methyl-parathion (MPT) and 4-nitrophenol (PNP) by a new type p-NiTSPc/p-PPD coated carbon fiber microelectrode (CFME), *Electroanalysis*, 2009, 21, 1167–1176.

4 A. Niazi and A. Yazdanipour, Spectrophotometric simultaneous determination of nitrophenol isomers by orthogonal signal correction and partial least squares, *J. Hazard. Mater.*, 2007, 146, 421–427.

5 A. Cladera, M. Miró, J. M. Estela and V. Cerdà, Multicomponent sequential injection analysis determination of nitro-phenols in waters by on-line liquid-liquid extraction and preconcentration, *Anal. Chim. Acta*, 2000, 421, 155–166.

6 X. Y. Liu, Y. S. Ji, Y. H. Zhang, H. X. Zhang and M. C. Liu, Oxidized multiwalled carbon nanotubes as a novel solid-phase microextraction fiber for determination of phenols in aqueous samples, *J. Chromatogr. A*, 2007, 1165, 10–17.

7 M. Mei, X. J. Huang, J. Yu and D. X. Yuan, Sensitive monitoring of trace nitrophenols in water samples using multiple monolithic fiber solid phase microextraction and liquid chromatographic analysis, *Talanta*, 2015, 134, 89–97.

8 H. Bagheri, A. Mohammadi and A. Salemi, On-line trace enrichment of phenolic compounds from water using a pyrrole-based polymer as the solid-phase extraction

View Article Online
DOI: 10.1039/C6EN00395H

sorbent coupled with high-performance liquid chromatography, *Anal. Chim. Acta*, 2004, 513, 445–449.

9 A. Mehdinia, S. Dadkhah, T. B. Kayyal and A. Jabbari, Design of a surface-immobilized 4-nitrophenol molecularly imprinted polymer via pre-grafting amino functional materials on magnetic nanoparticles, *J. Chromatogr. A*, 2014, 1364, 12–19.

10 A. Arvinte, M. Mahosenaho, M. Pinteala, A. M. Sesay and V. Virtanen, Electrochemical oxidation of p-nitrophenol using graphene-modified electrodes, and a comparison to the performance of MWNT-based electrodes, *Microchim Acta*, 2011, 174, 337–343.

11 P. S. Wang, J. Y. Xiao, M. M. Guo, Y. Xia, Z. L. Li, X. C. Jiang and W. Huang, Voltammetric determination of 4-nitrophenol at graphite nanoflakes modified glassy carbon electrode, *J. Electrochem. Soc.*, 2015, 162, 72–78.

12 X. F. Guo, Z. H. Wang and S. P. Zhou, The separation and determination of nitrophenol isomers by high-performance capillary zone electrophoresis, *Talanta*, 2004, 64, 135–139.

13 J. Fischer, J. Barek and J. Wang, Separation and detection of nitrophenols at capillary electrophoresis microchips with amperometric detection, *Electroanalysis*, 2006, 18, 195–199.

14 T. F. Hao, X. Wei, Y. J. Nie, Y. Q. Xu, Y. S. Yan, and Z. P. Zhou, An eco-friendly molecularly imprinted fluorescence composite material based on carbon dots for fluorescent detection of 4-nitrophenol, *Microchim. Acta*, 2016, 183, 2197–2203.

15 Y. Ma, G. Q. Pan, Y. Zhang, X. Z. Guo and H. Q. Zhang, Narrowly dispersed hydrophilic molecularly imprinted polymer nanoparticles for efficient molecular recognition in real aqueous samples including river water, milk, bovine serum, *Angew. Chem. Int. Ed.*, 2013, 52, 1511–1514.

View Article Online
DOI: 10.1039/C6EN00395H

16 S. H. Li, G. H. Yin, Q. Zhang, C. L. Li, J. H. Luo, Z. Xu and A. L. Qin, Selective detection of fenaminosulf via a molecularly imprinted fluorescence switch and silver nano-film amplification, *Biosens. Bioelectron.*, 2015, 71, 342–347.

17 S. F. Xu, H. Z. Lu, J. H. Li, X. L. Song, A. X. Wang, L. X. Chen and S. B. Han, Dummy molecularly imprinted polymers-capped CdTe quantum dots for the fluorescent sensing of 2,4,6-trinitrotoluene, *ACS Appl. Mater. Interfaces*, 2013, 5, 8146−8154.

18 X. Y. Wang, Q. Kang, D. Z. Shen, Z. Zhang, J. H. Li and L. X. Chen, Novel monodisperse molecularly imprinted shell for estradiol based on surface imprinted hollow vinyl-SiO_2 particles, *Talanta*, 2014, 124, 7–13.

19 J. X. Liu, Q. L. Deng, D. Y. Tao, K. G. Yang, L. H. Zhang, Z. Liang and Y. K. Zhang, Preparation of protein imprinted materials by hierarchical imprinting techniques and application in selective depletion of albumin from human serum, *Sci. Rep.*, 2014, 4, 5487–5492.

20 X. Y. Wang, J. L. Yu, Q. Kang, D. Z. Shen, J. H. Li and L. X. Chen, Molecular imprinting ratiometric fluorescence sensor for highly selective and sensitive detection of phycocyanin, *Biosens. Bioelectron.*, 2016, 77, 624–630.

21 S. E. Diltemiz, R. Say, S. Büyüktiryaki, D. Hür, A. Denizli and A. Ersöz, Quantum dot nanocrystals having guanosine imprinted nanoshell for DNA recognition, *Talanta*, 2008, 75, 890–896.

22 J. O. Winter, N. Gomez, S. Gatzert, C. E. Schmidt and B. A. Korgel, Variation of cadmium sulfide nanoparticle size and photoluminescence intensity with altered aqueous synthesis conditions, *Colloid Surf. A*, 2005, 254, 147–157.

23 X. Wang, P. T. Sheng, L. P. Zhou, X. Tong, L. Shi and Q. Y. Cai, Fluorescence immunoassay of octachlorostyrene based on Förster resonance energy transfer between CdTe quantum dots and rhodamine B, *Biosens. Bioelectron.*, 2014, 60, 52–56.

View Article Online
DOI: 10.1039/C6EN00395H

24 X. Y. Wang, J. L. Yu, X. Q. Wu, J. Q. Fu, Q. Kang, D. Z Shen, J. H. Li and L. X. Chen, A molecular imprinting-based turn-on ratiometric fluorescence sensor for highly selective and sensitive detection of 2,4-dichlorophenoxyaceticacid (2,4-D), *Biosens. Bioelectron.*, 2016, 81, 438–444.

25 X. H. Ren and L. G. Chen, Quantum dots coated with molecularly imprinted polymer as fluorescence probe for detection of cyphenothrin, *Biosens. Bioelectron.*, 2015, 64, 182–188.

26 Z. Zhang, J. H. Li, X. Y. Wang, D. Z. Shen and L. X. Chen, Quantum dots based mesoporous structured imprinting microspheres for the sensitive fluorescent detection of phycocyanin, *ACS Appl. Mater. Interfaces*, 2015, 7, 9118−9127.

27 L. X. Chen, X. Y. Wang, W. H. Lu, X. Q. Wu and J. H. Li, Molecular imprinting: perspectives and applications, *Chem. Soc. Rev.*, 2016, 45, 2137–2211.

28 W. Zhang, W. Liu, P. Li, H. B. Xiao, H. Wang and B. Tang, A fluorescence nanosensor for glycoproteins with activity based on the molecularly imprinted spatial structure of the target and boronate affinity, *Angew. Chem. Int. Ed.*, 2014, 53, 12489–12493.

29 X. Wei, T. F. Hao, Y. Q. Xu, K. Lu, H. J. Li, Y. S. Yan and Z. P. Zhou, Facile polymerizable surfactant inspired synthesis of fluorescent molecularly imprinted composite sensor via aqueous CdTe quantum dots for highly selective detection of λ-cyhalothrin, *Sens. Actuators B*, 2016, 224, 315–324.

30 H. F. Wang, Y. He, T. R. Ji and X. P. Yan, Surface molecular imprinting on Mn-doped ZnS quantum dots for room-temperature phosphorescence optosensing of pentachlorophenol in water, *Anal. Chem.*, 2009, 81, 1615–1621.

31 M. Rahman and H. J. Harmon, Absorbance change and static quenching of fluorescence of meso-tetra(4-sulfonatophenyl)porphyrin (TPPS) by trinitrotoluene (TNT), *Spectrochim. Acta Part A*, 2006, 65, 901–906.

View Article Online
DOI: 10.1039/C6EN00395H

32 C. Wang, Q. Ma, W. Dou, S. Kanwal, G. Wang, P. Yuan and X. Su, Synthesis of aqueous CdTe quantum dots embedded silica nanoparticles and their applications as fluorescence probes, *Talanta*, 2009, 77, 1358–1364.

33 E. B. Ying, D. Li, S. J. Guo, S. J. Dong and J. Wang, Synthesis and bio-imaging application of highly luminescent mercaptosuccinic acid-coated CdTe nanocrystals, *PLoS ONE*, 2008, 3, e2222.

34 D. Y. Li, X. W. He, Y. Chen, W. Y. Li and Y. K. Zhang, Novel hybrid structure silica/CdTe/molecularly imprinted polymer: synthesis, specific recognition, and quantitative fluorescence detection of bovine hemoglobin, *ACS Appl. Mater. Interfaces*, 2013, 5, 12609−12616.

35 G. H. G. Ahmed, R. B. Laíño, J. A. G. Calzón and M. E. D. García, Highly fluorescent carbon dots as nanoprobes for sensitive and selective determination of 4-nitrophenol in surface waters, *Microchim. Acta*, 2015, 182, 51–59.

36 W. Li, H. R. Zhang, S. Chen, Y. L. Liu, J. L. Zhuang and B. F. Lei, Synthesis of molecularly imprinted carbon dot grafted YVO_4:Eu^{3+} for the ratiometric fluorescent determination of paranitrophenol, *Biosens. Bioelectron.*, 2016, 86, 706–713.

37 Y. Zhou, Z. B. Qu, Y. B. Zeng, T. S. Zhou and G. Y. Shi, A novel composite of grapheme quantum dots and molecularly imprinted polymer for fluorescent detection of paranitrophenol, *Biosens. Bioelectron.*, 2014, 52, 317–323.

38 X. Wei, Z. P. Zhou, T. F. Hao, H. J. Li, Y. Z. Zhu, L. Gao and Y. S. Yan, A novel molecularly imprinted polymer thin film at surface of ZnO nanorods for selective fluorescence detection of para-nitrophenol, *RSC Adv.*, 2015, 5, 44088–44095.

39 J. X. Liu, H. Chen, Z. Lin and J. M. Lin, Preparation of surface imprinting polymer capped Mn-doped ZnS quantum dots and their application for chemiluminescence detection of 4-nitrophenol in tap water, *Anal. Chem.*, 2010, 82, 7380–7386.

View Article Online
DOI: 10.1039/C6EN00395H

Table 1. Spiked recoveries and RSDs (%, *n*=3) for the determination of 4-NP in seawater and lake water samples using the QD@MIPs sensor.

Sample	Added (μM)	Found (μM)	Recovery[a]±RSD (%)
Seawater	0	0	–
	0.400	0.424	106.0±3.2
	0.800	0.825	103.1±4.8
	1.000	0.927	92.7±3.1
Lake water	0	0	–
	0.400	0.437	109.2±4.7
	0.800	0.860	107.5±3.5
	1.000	1.023	102.3±3.4

[a] Average value from three individual experiments.

Table 2. Performance comparison with other reported methods for 4-NP sensing.

System	Mechanism	Linear range (μM)	LOD (μM)	IF[a]	Real sample	Ref.
C-dots[b]	Energy transfer from C-dots to 4-NP	0.1–50	0.028	–	River water	35
MIP-coated carbon dot incorporated with YVO_4: Eu^{3+}[c] nanoparticles	Fluorescence resonance energy transfer (FRET) and photoinduced eletron transfer (PET) between CDs and 4-NP	0–12	0.150	–	Tap water, urine samples	36
MIP-coated GQDs[d]	Electron transfer from GQDs to 4-NP	0.14–21	0.064	2.2	Tap water, river water	37
MIP-capped ZnO nanorods	–	0.5–14	0.036	5.918	River water	38
MIP-capped Mn-doped ZnS QDs	Electron transfer from Mn-doped ZnS QDs to 4-NP	0.1–40	0.076	2.113	Tap water	39
MIP-C-dots	Electron transfer from C-dots to 4-NP	0.2–50	0.060	2.76	River water	14
MIP-coated AMA-modified QDs	Electron transfer from AMA-modified QDs to 4-NP	0.2–8	0.051	9.1	Seawater, lake water	This work

[a] Iimprinting factor. [b] Carbon dots. [c] Eu^{3+}-activated yttrium orthovanadate. [d] Graphene quantum dots.

View Article Online
DOI: 10.1039/C6EN00395H

Figure caption

Fig. 1. Schematic illustration for the preparation process and possible detection principle of QD@MIPs nanosensor.

Fig. 2. Fluorescence spectra of (a) QDs, (b) AMA-modified CdTe QDs, and (c) QD@MIPs.

Fig. 3. FT-IR spectra of (a) QDs, (b) QD@MIPs, and (c) QD@NIPs.

Fig. 4. (A) Effect of pH on fluorescence intensities of QD@MIPs in the presence of 2 μM 4-NP. (B) Fluorescence response time of QD@MIPs for 4-NP. The fluorescence intensity was recorded at the wavelength of 549 nm.

Fig. 5. Fluorescence spectra of (A) QD@MIPs, and (B) QD@NIPs with addition of the different concentrations of 4-NP (0–8 μM). The inset graphs show the Stern−Volmer plots for (A) QD@MIPs, and (B) QD@NIPs. Experimental conditions: concentration of QD@MIPs or QD@NIPs was 0.02 mg·mL^{-1}; excited light, 420 nm; silt widths of excitation and emission, 6 nm.

Fig. 6. Fluorescence quenching amounts of QD@MIPs and QD@NIPs for 4-NP and its analogues (upper), respectively, and the chemical structures of 4-NP and its analogues (below). Experimental conditions: concentration of QD@MIPs or QD@NIPs, 0.02 mg·mL^{-1}; 4-NP and its analogues, 2 μM respectively; excited light, 420 nm; silt widths of excitation and emission, 6 nm.

View Article Online
DOI: 10.1039/C6EN00395H

Fig. 1.

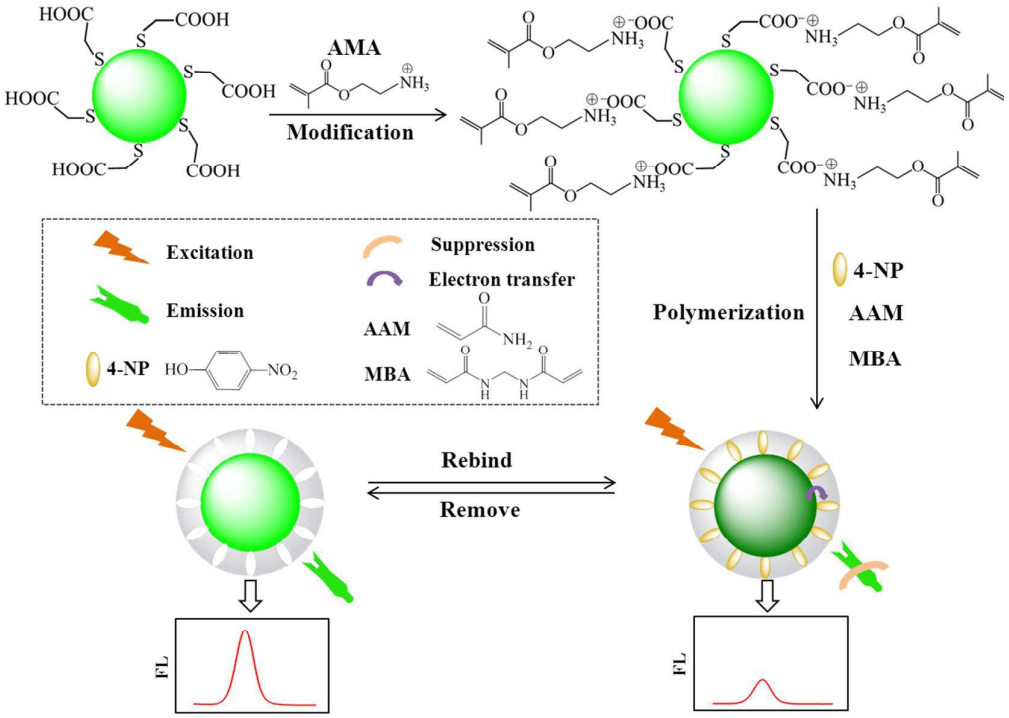

View Article Online
DOI: 10.1039/C6EN00395H

Fig. 2.

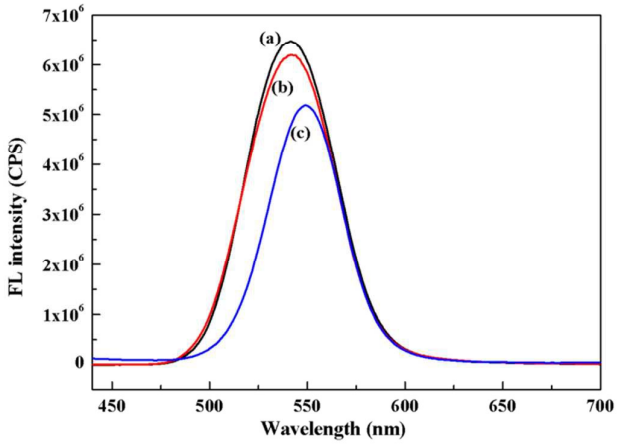

View Article Online
DOI: 10.1039/C6EN00395H

Fig. 3.

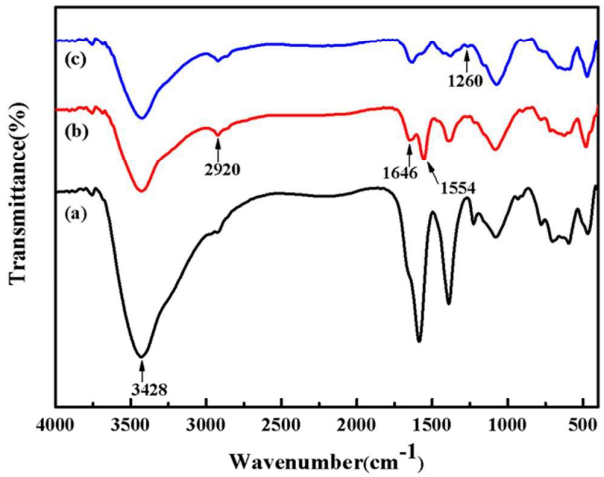

View Article Online
DOI: 10.1039/C6EN00395H

Fig. 4.

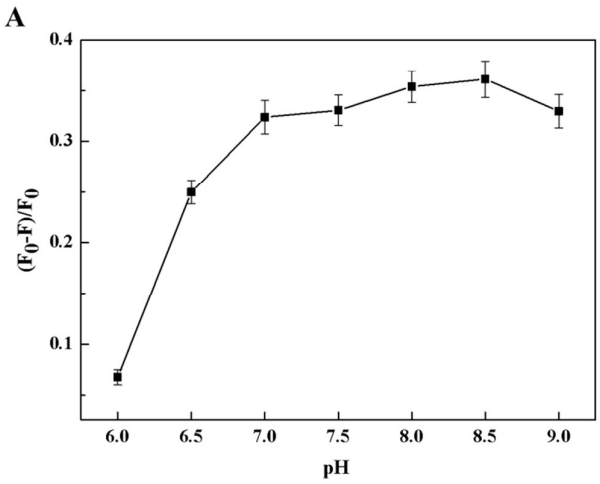

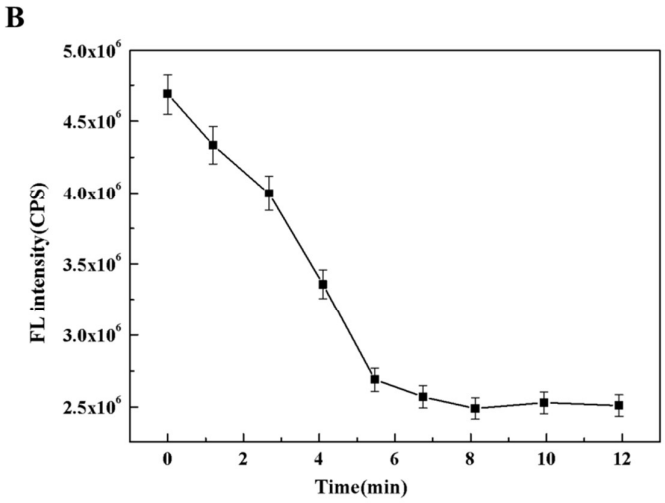

View Article Online
DOI: 10.1039/C6EN00395H

Fig. 5.

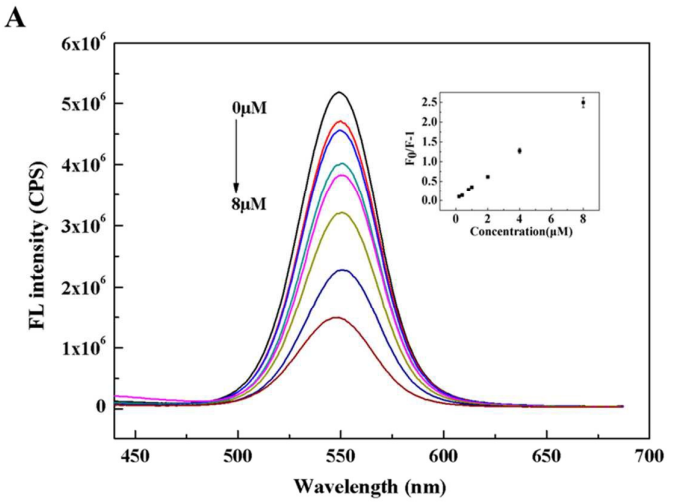

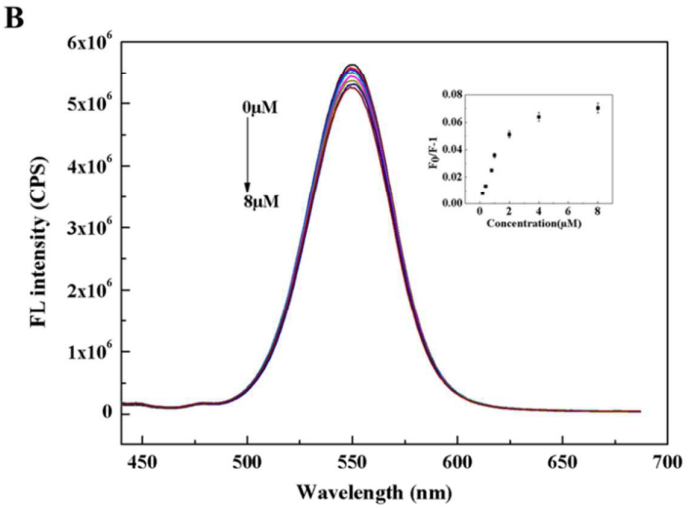

View Article Online
DOI: 10.1039/C6EN00395H

Fig. 6.

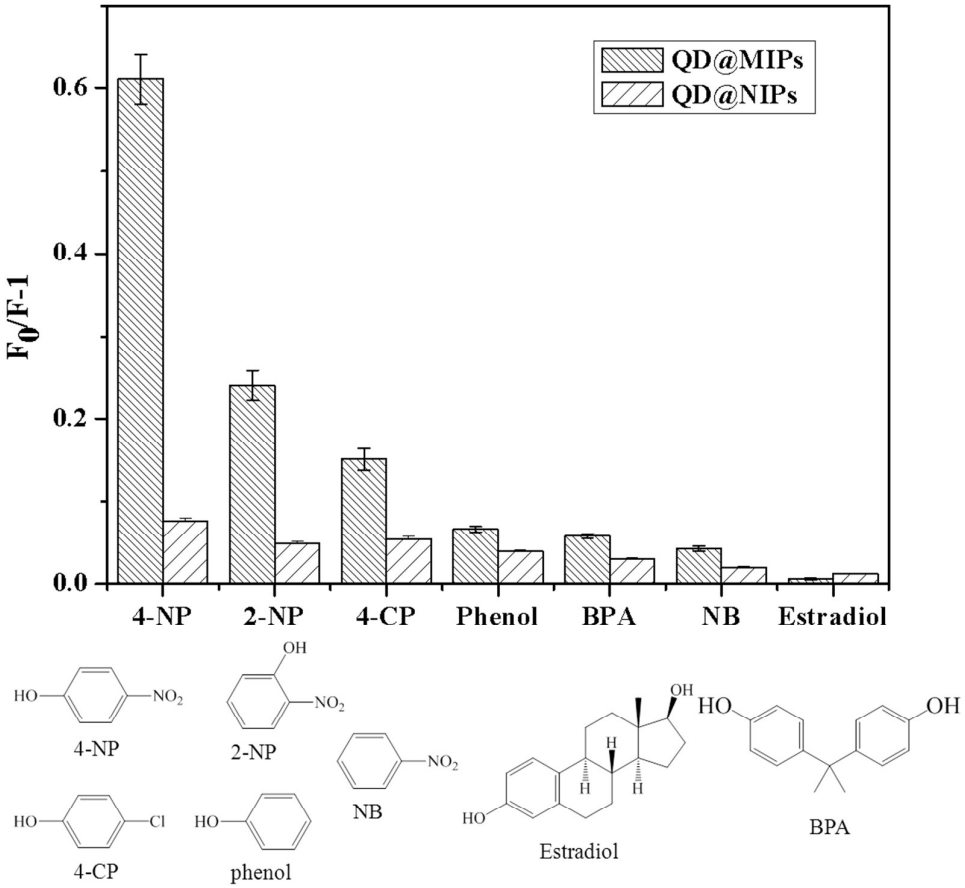

View Article Online
DOI: 10.1039/C6EN00395H

A table of contents entry

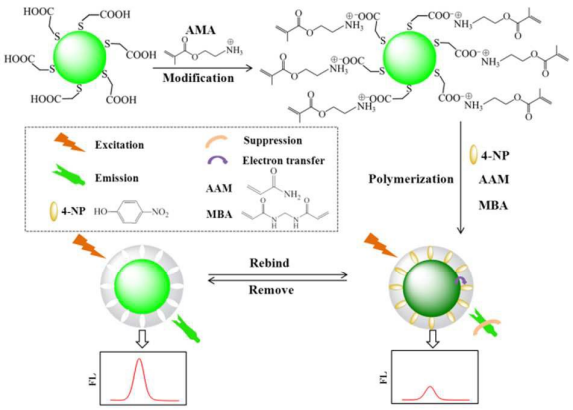

A facile surface imprinting polymerization one-pot synthesis strategy based on electron-transfer induced fluorescence quenching mechanism for fluorescent detection of 4-nitrophenol.